



# UNIVERSITÀ DI TRENTO

DEPARTMENT OF PHYSICS

Master degree in Physics

---

## Chaos things

---

*Graduant:*  
Manuel BITTO

*Supervisor:*  
Leonardo RICCI

*Co-supervisor:*  
Alessio PERINELLI

24 October 2024



# Contents

<b>Introduction</b>	<b>v</b>
<b>1 An electronic analog of the Burridge-Knopoff model</b>	<b>1</b>
1.1 Mechanical Burridge-Knopoff model . . . . .	1
1.1.1 Motion of two coupled blocks . . . . .	2
1.1.2 Dimensionless system . . . . .	3
1.2 Electronic analog for the motion of two blocks . . . . .	3
1.3 Characterization of the single block behavior . . . . .	5
1.3.1 Breadboard implementation . . . . .	5
1.3.2 Integrated board implementation . . . . .	6
1.4 AAAAAAAAAAAAAAAAAAAAA . . . . .	7
1.5 Prototypes . . . . .	7
1.6 Board . . . . .	9
1.7 New board . . . . .	10
1.8 Conclusions . . . . .	10
<b>2 Chaos analysis of multiple oscillators</b>	<b>13</b>
2.1 Two blocks . . . . .	13
2.2 Three blocks . . . . .	14
2.3 Four blocks . . . . .	15
2.4 Five blocks . . . . .	16
2.5 Six blocks . . . . .	17
2.6 Seven blocks . . . . .	17
2.7 Eight blocks . . . . .	18
2.8 Nine blocks . . . . .	19
2.9 Ten blocks . . . . .	20
2.10 Conclusions . . . . .	20
<b>3 Earthquake properties and statistical model of a fault</b>	<b>21</b>
<b>Bibliography</b>	<b>23</b>



# Introduction

# Chapter 1

## An electronic analog of the Burridge-Knopoff model

### 1.1 Mechanical Burridge-Knopoff model

The Burridge-Knopoff (BK) spring-block model [1] is a two-dimensional system of massive blocks lying on a rough horizontal surface. Each block is connected to its nearest neighbors by a set of springs, and linked by another spring to an upper horizontal ceiling moving with constant velocity with respect to the lower plate, as shown in Fig. 1.1.

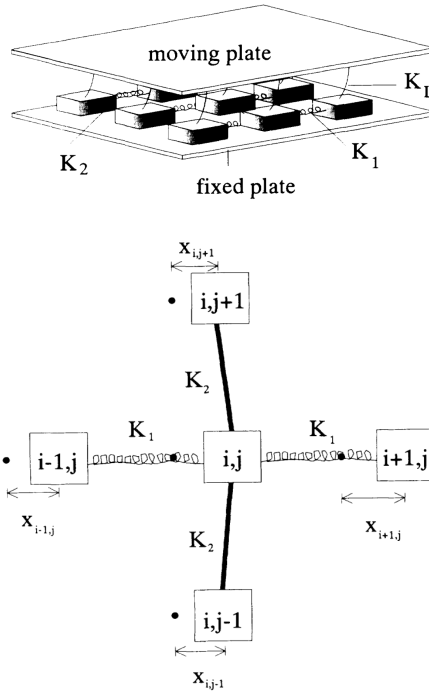


Figure 1.1: Visual representation of the Burridge-Knopoff spring-block model.  $K_1$  and  $K_2$  are the elastic constants, respectively, of the horizontal and vertical springs, while  $K_L$  is the elastic constant of the springs connecting the blocks and the moving plate. The figure below represents the interaction between a block and its four nearest neighbors, as a function of the displacement  $x_{i,j}$ . Figure adapted from Ref. [2].

The blocks are driven by the relative movement of the two rigid plates. When the force on one block reaches some threshold value  $F_{\text{th}}$ , the block slips, and it is reasonable to assume that the force on that block becomes zero. Then, the force on the four nearest neighbors is increased, often resulting in further slips, and an avalanche can occur.

The purpose of the BK model is the description of the dynamical behavior of real faults, whereby a constant, slow driving motion of plates produces an accumulation of “stress” up to a threshold at which such stress is released through an abrupt motion – i.e., an earthquake – of one or more of the system’s constituent parts.

### 1.1.1 Motion of two coupled blocks

The mechanical BK model for the motion of two coupled blocks is shown schematically in Fig. 1.2. The upper ceiling moves with respect to the surface with a constant velocity  $u_d$ . Let  $x_1, x_2$  be the displacements of the block positions relative to a state in which the springs are relaxed, and  $u_1, u_2$  the velocities of the blocks in the lower surface frame, so that  $u_i = u_d + \dot{x}_i$  with  $i = 1, 2$ .

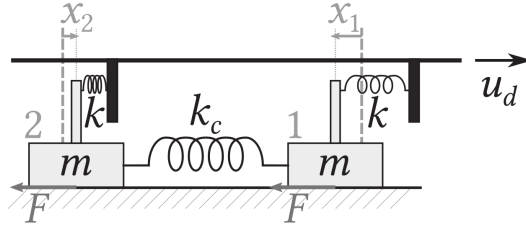


Figure 1.2: Two-blocks mechanical BK model. The upper ceiling, which the blocks are coupled to via springs with elastic constant  $k$ , is dragged with constant velocity  $u_d$  with respect to the underlying surface. This surface exerts a nonlinear, velocity-dependent friction  $F$  to each block’s motion. Figure adapted from Ref. [3].

The equations of motion are thus given by

$$\begin{aligned}
 m \frac{du_1}{dt} &= -kx_1 - k_c(x_1 - x_2) - F(u_1), \\
 \frac{dx_1}{dt} &= u_1 - u_d, \\
 m \frac{du_2}{dt} &= -kx_2 - k_c(x_2 - x_1) - F(u_2), \\
 \frac{dx_2}{dt} &= u_2 - u_d,
 \end{aligned} \tag{1.1}$$

where  $m$  is the mass of the blocks,  $k$  is the elastic constant of the springs that connect the blocks to the ceiling,  $k_c$  is the elastic constant of the spring linking the two blocks, and  $F(u)$  is the nonlinear velocity-dependent friction. The velocities are assumed to be non-negative.

### 1.1.2 Dimensionless system

It is possible to render this system dimensionless by defining the following dimensionless quantities ( $i$  takes the values 1 and 2): a time  $\tau \equiv t\sqrt{k/m}$ , a velocity  $\nu_i \equiv u_i/u_0$ , a position  $\xi_i \equiv x_i\sqrt{k/m}/u_0$ , a friction  $\varphi(\nu_i) \equiv F(\nu_i)/(u_0\sqrt{mk})$  and a parameter  $\lambda \equiv k_c/k$ . The four equations of motion can then be written as

$$\begin{aligned}\frac{d\nu_i}{d\tau} &= -(1 + \lambda)\xi_i + \lambda\xi_{3-i} - \varphi(\nu_i), \\ \frac{d\xi_i}{d\tau} &= \nu_i - \nu_d.\end{aligned}\tag{1.2}$$

There exists a relative freedom in the choice of the friction  $\varphi(\nu)$ , provided that (i)  $\varphi(\nu < 0) = 0$ , (ii)  $\varphi(\nu \geq 0) \geq 0$  and (iii)  $\varphi(\nu)$  decreases down to zero from a maximum value  $\varphi(0)$  that occurs at  $\nu = 0$ .

It is useful to define the equations of motion also in the case of a lower surface moving with a positive dimensionless velocity  $\Delta\nu$ , so that  $\nu'_i = \nu_i + \Delta\nu$  and  $\nu'_d = \nu_d + \Delta\nu$ . The system of equations becomes:

$$\begin{aligned}\frac{d\nu'_i}{d\tau} &= -(1 + \lambda)\xi_i + \lambda\xi_{3-i} - \varphi(\nu'_i - \Delta\nu), \\ \frac{d\xi_i}{d\tau} &= \nu'_i - \nu'_d.\end{aligned}\tag{1.3}$$

## 1.2 Electronic analog for the motion of two blocks

In order to analyze the properties of the BK model, it is possible to build an electronic circuit which differential equations are the same as Eqs. 1.3. The first implementation was done by Field, Venturi and Nori [4] by drawing a direct parallelism between mechanical and electrical quantities. The idea was to use capacitance as mass, inductance as the reciprocal of elastic constant, voltage as velocity and current as position. However, this implementation has two main drawbacks. The first one is the usage of inductances, which are typically bulky and have intrinsically large tolerances compared with other components, resulting in higher uncertainties; moreover, their tunability is very low. The second issue is that the current is a state variable, and it is less straightforward to measure it with respect to voltage.

It is possible to use another implementation [3] which does not rely on inductances and uses only voltages as state variables. In order to do so it is necessary to rewrite the system equations as integral equations, so that they can be implemented by electronic integrators that are more stable than the differentiators. The new state variables are defined as  $V_i \equiv \nu_i V_0$  and  $W_i \equiv \xi_i V_0$  and the new time constant is given by  $\tau = RC$ , where  $R$  and  $C$  are suitably chosen resistance and capacitance. Integrating the system of Eqs. 1.3 for a moving surface and replacing  $V'_i \equiv V_i + \Delta V$  and  $V'_d \equiv V_d + \Delta V$ , where  $V_d \equiv V_0\nu_d$  and  $\Delta V \equiv V_0\Delta\nu$ , leads to the following system of equations:



$$V_i + \Delta V = -\frac{1}{RC} \int \left[ (1 + \lambda)W_i - \lambda W_{3-i} + V_0 \varphi \left( \frac{V_i}{V_0} \right) \right] dt, \quad (1.4)$$

$$W_i = -\frac{1}{RC} \int (V_d - V_i) dt,$$

where  $\lambda = R/R_c$  and  $R_c$  is a suitably chosen resistance.

These differential equations are implemented by the circuit shown in Fig. 1.3, which makes use of resistors, capacitors, diodes and operational amplifiers, without any inductance. Assuming for a while that  $\Delta V$  and the nonlinear element  $\varphi(V_i/V_0)$  were not present, the two integrations above could be promptly implemented by considering the black part of the circuit diagram.

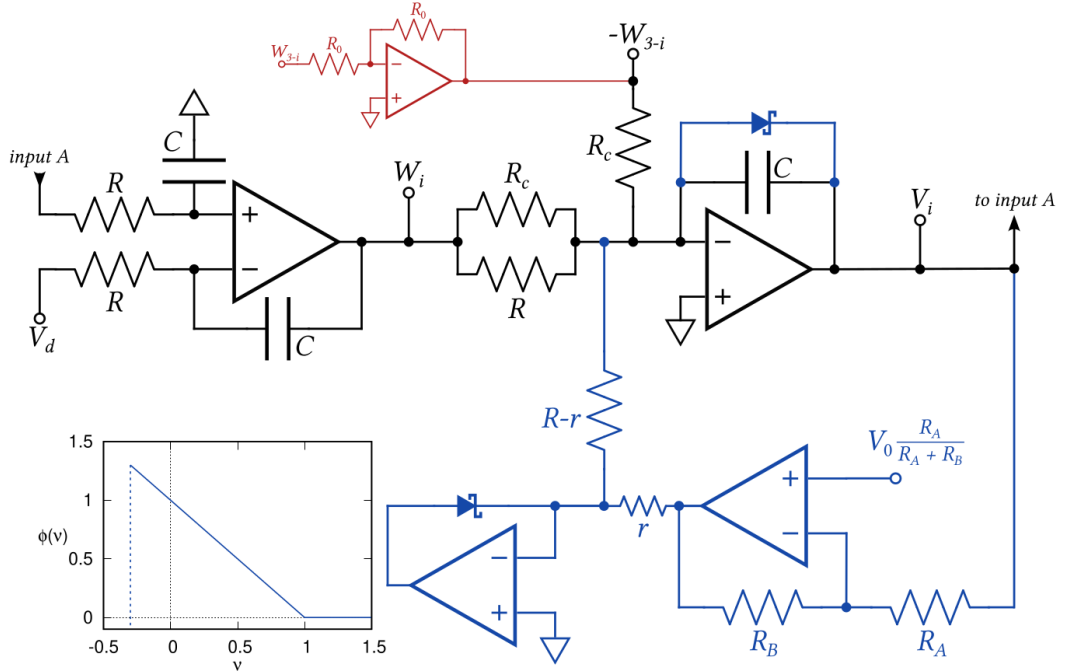


Figure 1.3: Inductorless representation of the BK model. The circuit diagram refers to a single block, labeled by  $i = 1, 2$ . The bottom left plot shows the characteristic of the nonlinear element, i.e. the blue part of the diagram. The red part is a standard inverting operational amplifier, which is necessary for the coupling between two blocks. Figure adapted from Ref. [3].

The nonlinear term is instead represented by the blue part of the diagram and it is implemented as follows. A Schottky diode is inserted on the feedback network on the integrator producing  $V_i$ ; this ensures that  $V_i$  does not drop below  $-V_{\text{diode}}$ , where  $V_{\text{diode}} \approx 0.3$  V. In order to not contradict the constraint that the “velocity” must be always non-negative, it is necessary to set  $\Delta V = V_{\text{diode}}$ . In this way the first of the constraints set in Sec. 1.1.2, i.e.  $\varphi(V_i < 0) = 0$  is satisfied, since the voltage cannot drop below zero.

The nonlinear friction element consists in a linear drop for the analog of the velocity-weakening force, and it is implemented using two additional op-amps as

follows. The output of the first op-amp is given by  $V_0 - V_i R_B / R_A$ . Downstream of the resistor  $r$ , this voltage is prevented to drop below zero by an active clamp made of the second op-amp which has a diode in its feedback network. The resulting voltage is fed back into the integrator generating  $V_i$  through an additional resistor  $R - r$ .

### 1.3 Characterization of the single block behavior

With the aim of analyzing the circuit represented in Fig. 1.3, it is necessary to characterize its behavior. The first characterization concerns the function of a single block, in the absence of couplings. In this case  $\lambda = 0$  and the differential equations of the system can be simplified as (the subscript  $i$  is omitted):

$$\begin{aligned} \frac{d^2 V}{dt^2} + \frac{1}{\tau} \varphi' \left( \frac{V}{V_0} \right) \frac{dV}{dt} + \frac{1}{\tau^2} (V - V_d) &= 0 \\ \frac{dW}{dt} &= \frac{1}{\tau} (V - V_d) \end{aligned} \tag{1.5}$$

where  $\varphi'$  is the derivative of the friction with respect to the velocity  $V$ . The equation for the velocity is of the kind met in the classical description of stick-slip vibrations [5], i.e. of the self-sustained oscillations induced by friction. This means that a sinusoidal-like behavior for  $V$  and  $W$  has to be expected.

In order to check the validity of these equations, the circuit was physically implemented in two different manners. The first implementation was done on a breadboard using large electronic components; the main issue with this system is that it is not scalable, due to the fact that a single circuit occupies half of the entire space on the breadboard. The second one consists instead in an integrated board in which 25 circuits like the one in Fig. 1.3 were implemented; the scalability issue is solved in this case, so that this board could be utilized to study the behavior of many coupled blocks, as will be done in Chapter 2.

#### 1.3.1 Breadboard implementation

The breadboard implementation was made using 1N5817 Schottky diodes and OP27 op-amps; these op-amps were supplied with  $V_{CC} = \pm 12$  V. The nominal values for the resistances and capacitors are  $R = R_c = 10$  k $\Omega$ ,  $R_A = R_B = 10$  k $\Omega$ ,  $r = 1.8$  k $\Omega$  and  $C = 100$  nF, so that the characteristic time of the circuit is  $\tau = 1$  ms. The input voltages are  $V_0 = 1$  V and the variable voltage  $V_d$ , while the output voltages are  $V$  and  $W$  (the subscript  $i$  is omitted).

The single block behavior of this circuit is shown in Fig. 1.4. As expected by Eqs. 1.5, both the velocity  $V$  and the position  $W$  exhibit an oscillating behavior. While  $W$  closely resembles a sinusoidal wave,  $V$  possesses a lower clamping that makes it different from a simple periodic wave; this clamping is due to the presence of the Schottky diodes, which prevent the velocity to become negative, as discussed in Sec. 1.2. In the end, both the frequency and the amplitude of the waves depend on the driving voltage  $V_d$ .

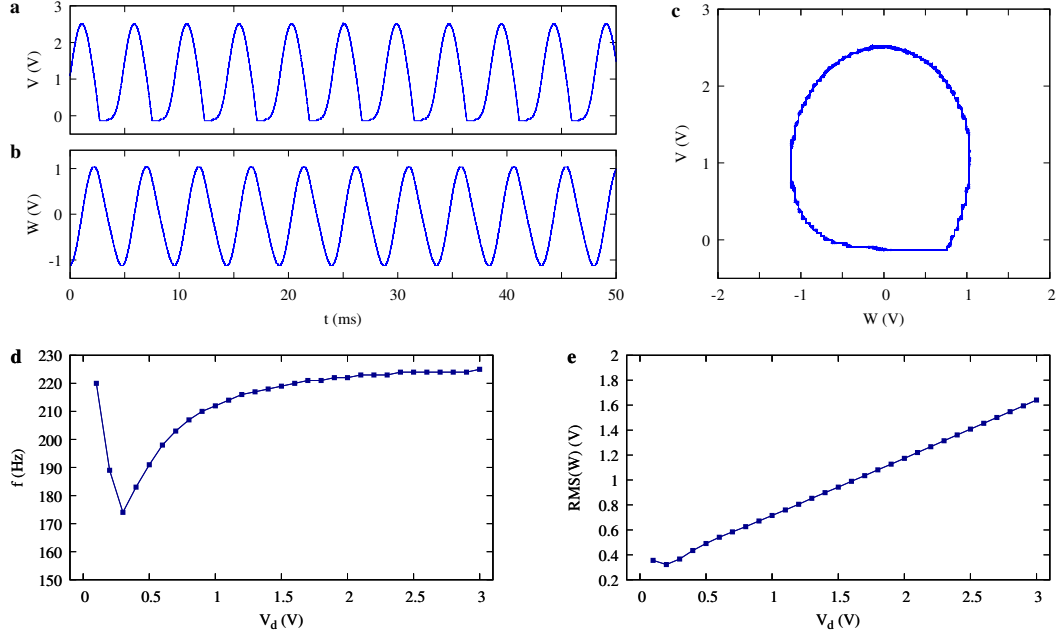


Figure 1.4: Oscillating behavior for the circuit implemented on the breadboard. (a) Plot of  $W$  and (b) of  $V$  as a function of time, for  $V_d = 1$  V. (c) Phase portrait (Lissajous figure) of  $V$  versus  $W$ . (d) Frequency and (e) root mean square amplitude of the output signal  $W$  as a function of the parameter  $V_d$ .

### 1.3.2 Integrated board implementation

The circuit diagram for each of the 25 chips on the integrated board is equivalent to the one shown in Fig. 1.3. The only differences with the breadboard implementation concern the nonlinear components, i.e. the use of DFLS1100 Schottky diodes and quad operational amplifiers OP470, which offer comparable performances to the components used in the previous section, i.e. 1N5817 Schottky diodes and OP27 op-amps.

The single block behavior of this circuit is shown in Fig. 1.8.

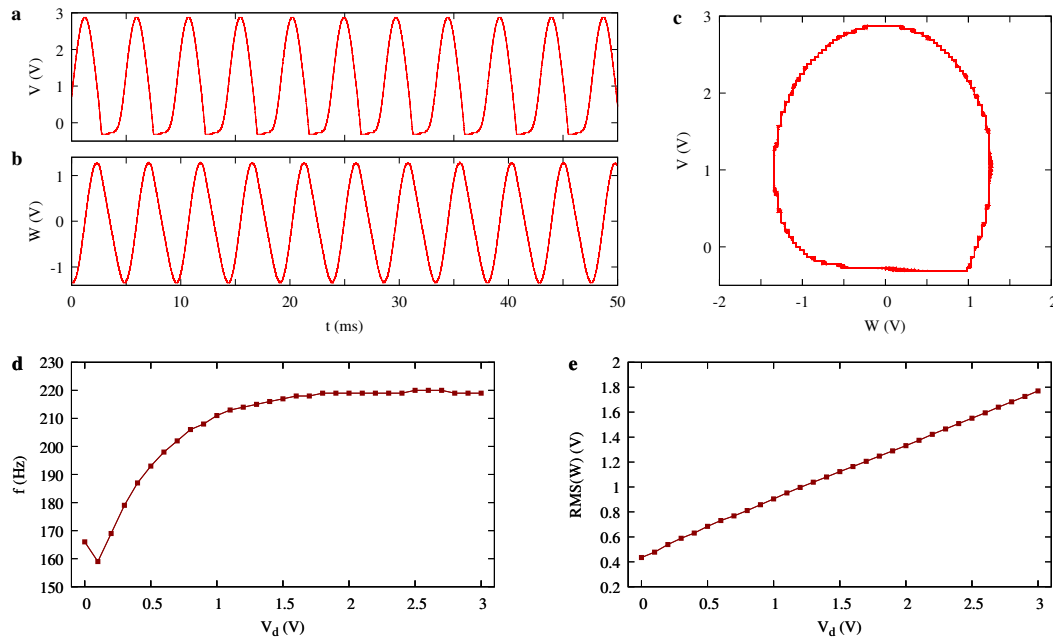


Figure 1.5: Oscillating behavior for the circuit implemented on the integrated board. (a) Plot of  $W$  and (b) of  $V$  as a function of time, for  $V_d = 1$  V. (c) Phase portrait (Lissajous figure) of  $V$  versus  $W$ . (d) Frequency and (e) root mean square amplitude of the output signal  $W$  as a function of the parameter  $V_d$ .

## 1.4 AAAAAAAAAAAAAAAAAAAAAA

### 1.5 Prototypes

In order to describe the coupling between many oscillators it is not possible use the breadboard implementation of the circuit shown in Fig. 1.3, due to scalability issues. For the purpose of improving the system scalability, two smaller prototypical chips have been built. The circuit implemented in each chip is shown in Fig. 1.6. The differences between this circuit and the one used in the previous section lie in the nonlinear elements; in this case MBRA210L Schottky diodes have been used, as well as quad operational amplifiers OP470, which offer comparable performance to OP27 op-amps.

The oscillating behavior of this circuit is shown in Fig. 1.7 for both chips. These systems are much less stable with respect to the circuit implemented on the breadboard; in fact, measurements were possible only in a small range for  $V_d$ , namely  $V_d \leq 1.1$  V for one chip and  $V_d \leq 0.6$  V for the other one. It is also important to point out that the diode clamping is not present; in fact, it is only noticeable at voltages  $V_d \lesssim 0.4$  V.

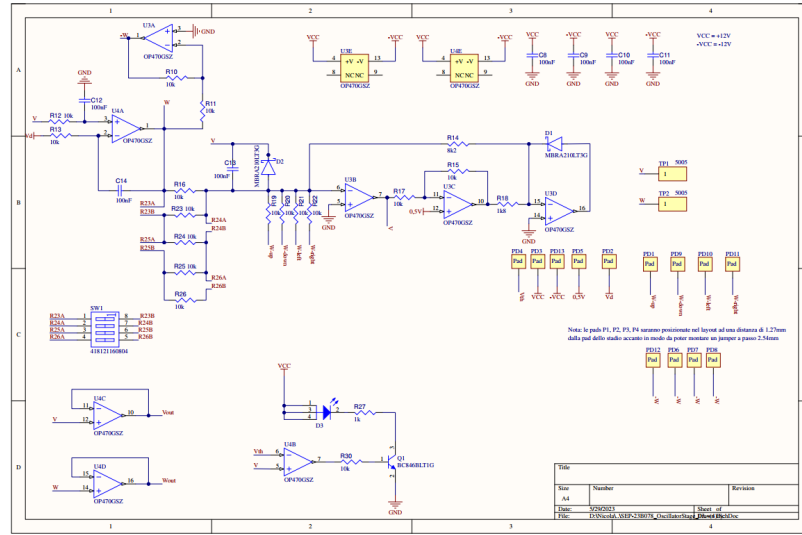


Figure 1.6: Circuit diagram of one prototypical chip.

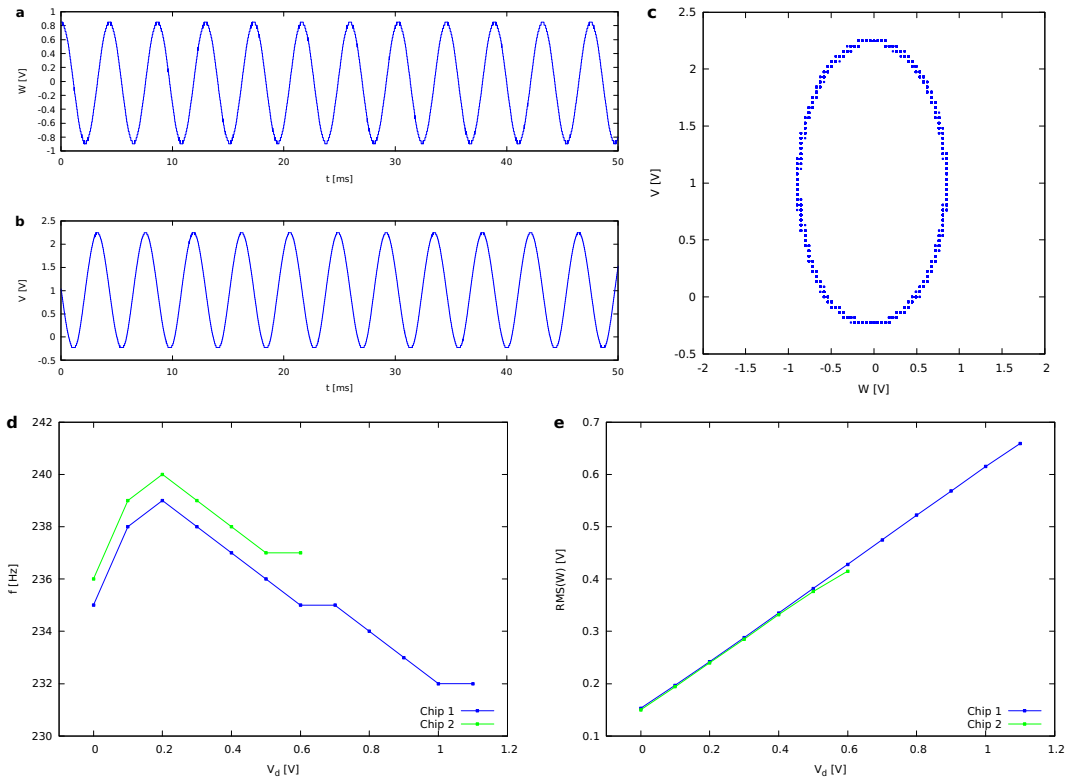


Figure 1.7: Oscillating behavior for the circuit implemented on the prototypical chips. (a) Plot of  $W$  and (b) of  $V$  as a function of time, for  $V_d = 1$  V. (c) Phase portrait (Lissajous figure) of  $V$  versus  $W$ . (d) Frequency and (e) root mean square amplitude of the output signal  $W$  as a function of the parameter  $V_d$  and for the two different chips.

## 1.6 Board

In order to finally analyze the behavior of many coupled oscillators, a board containing 25 chips (or blocks) has been built. The circuit diagram is equivalent to the one shown in Fig. 1.6 for the prototypes, the only difference being the use of DFLS1100 Schottky diodes instead of MBRA210L ones.

The oscillating behavior is shown in Fig. 1.8. Once again, these systems are not as stable as the circuit on the breadboard; measurements were in fact taken for  $V_d \leq 2.2$  V for the first two blocks. It is important to notice that in the voltage range  $0.6 \text{ V} \leq V_d \leq 2.1 \text{ V}$  a clamping of the output voltage  $V$  can be observed; this is not intended and is probably due to intrinsic limitations in the current.

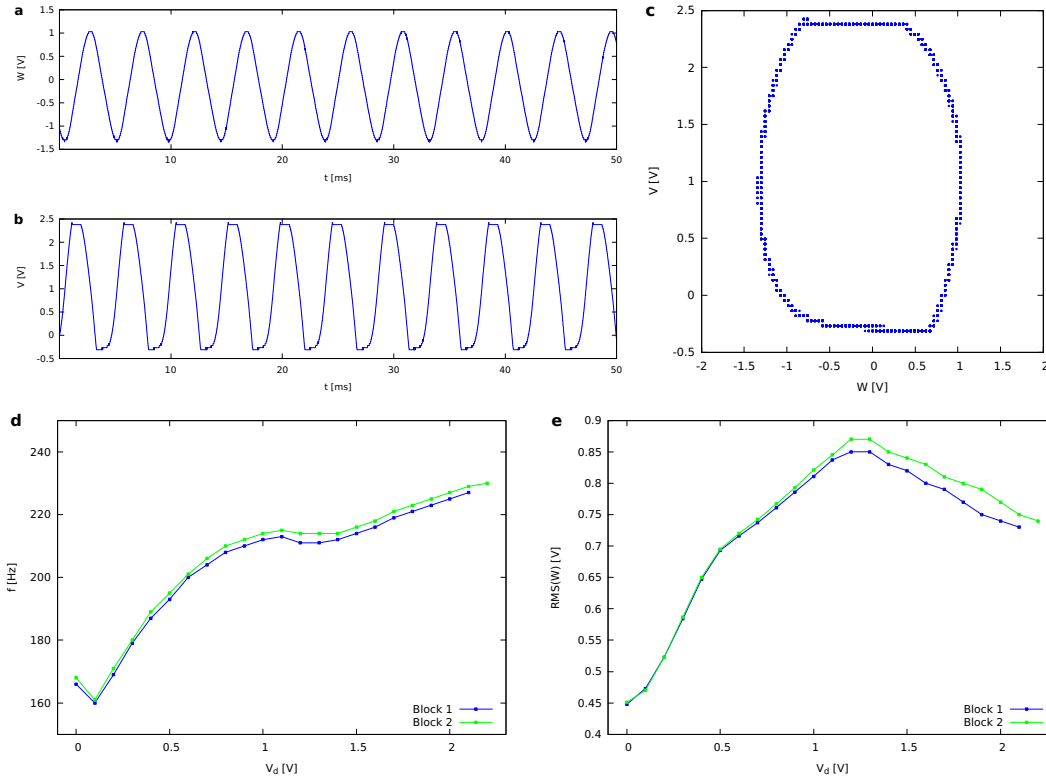


Figure 1.8: Oscillating behavior for the circuit implemented on the board. (a) Plot of  $W$  and (b) of  $V$  as a function of time, for  $V_d = 1$  V. (c) Phase portrait (Lissajous figure) of  $V$  versus  $W$ . (d) Frequency and (e) root mean square amplitude of the output signal  $W$  as a function of the parameter  $V_d$  and for two different blocks.

## 1.7 New board

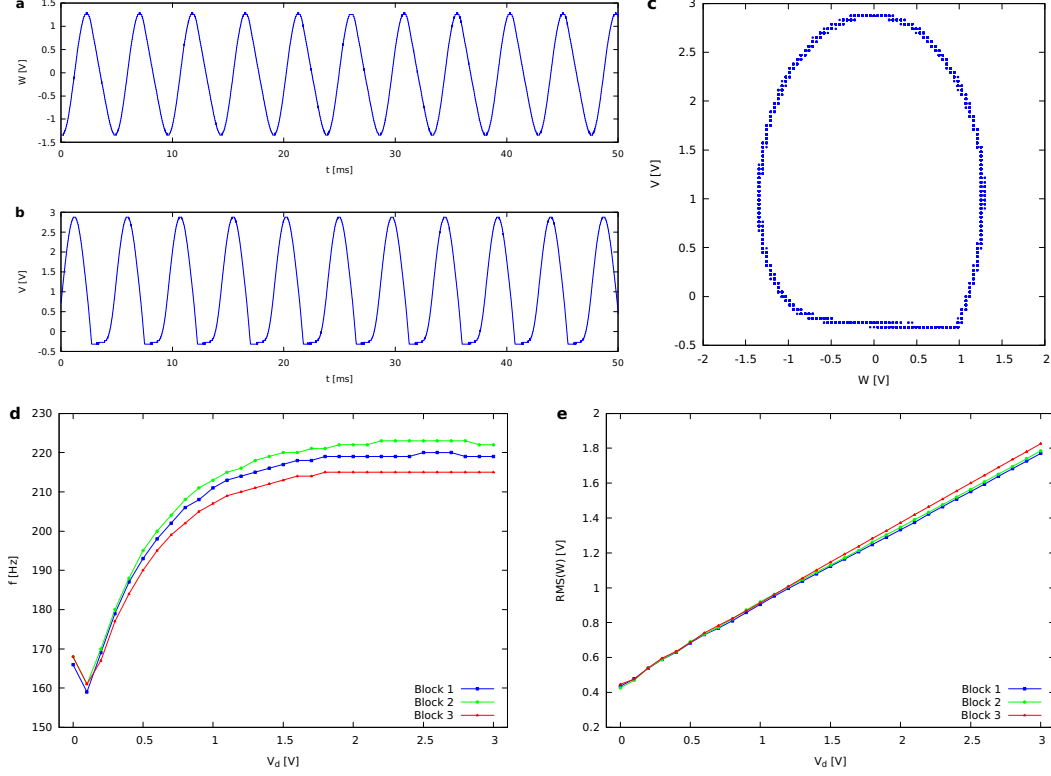


Figure 1.9: Oscillating behavior for the circuit implemented on the new board. (a) Plot of  $W$  and (b) of  $V$  as a function of time, for  $V_d = 1$  V. (c) Phase portrait (Lissajous figure) of  $V$  versus  $W$ . (d) Frequency and (e) root mean square amplitude of the output signal  $W$  as a function of the parameter  $V_d$  and for three different blocks.

## 1.8 Conclusions

The comparison between frequency and amplitude on the three implementations is shown in Fig. 1.10. The frequency of the board is very similar to the breadboard one for voltages  $V_d < 1$  V; at higher voltages there are small deviations in the board, probably due to the increased relevance of the current clamping. This might also be the reason why the amplitude behavior of the board is not linear.

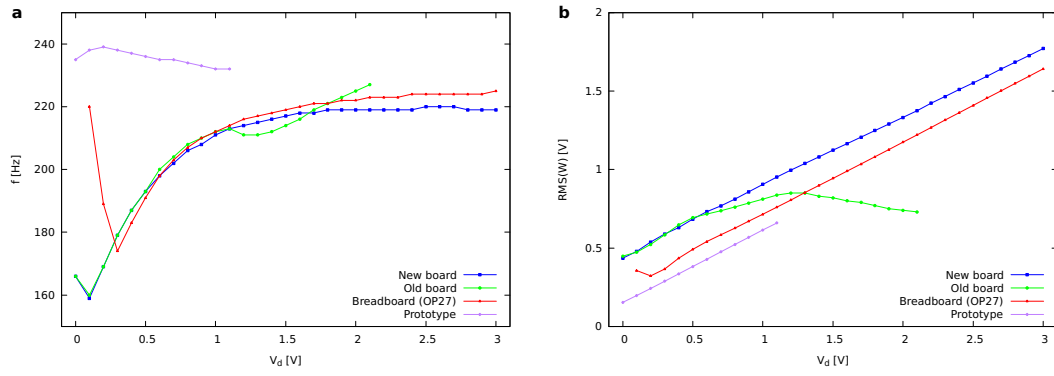


Figure 1.10: (a) Frequency and (b) root mean square amplitude of the output signal  $W$  as a function of the parameter  $V_d$  for the three implementations of the BK model, i.e. the first block of the board, the breadboard implementation with the OP27 op-amps and the first prototypical chip.





## Chapter 2

# Chaos analysis of multiple oscillators

### 2.1 Two blocks

The coupling between two oscillators is performed by connecting the inverted voltage  $-W_2$  of the second oscillator to the first one and viceversa, as shown in Fig. ???. A chaotic behavior can be observed, as can be seen in Fig. 2.1.

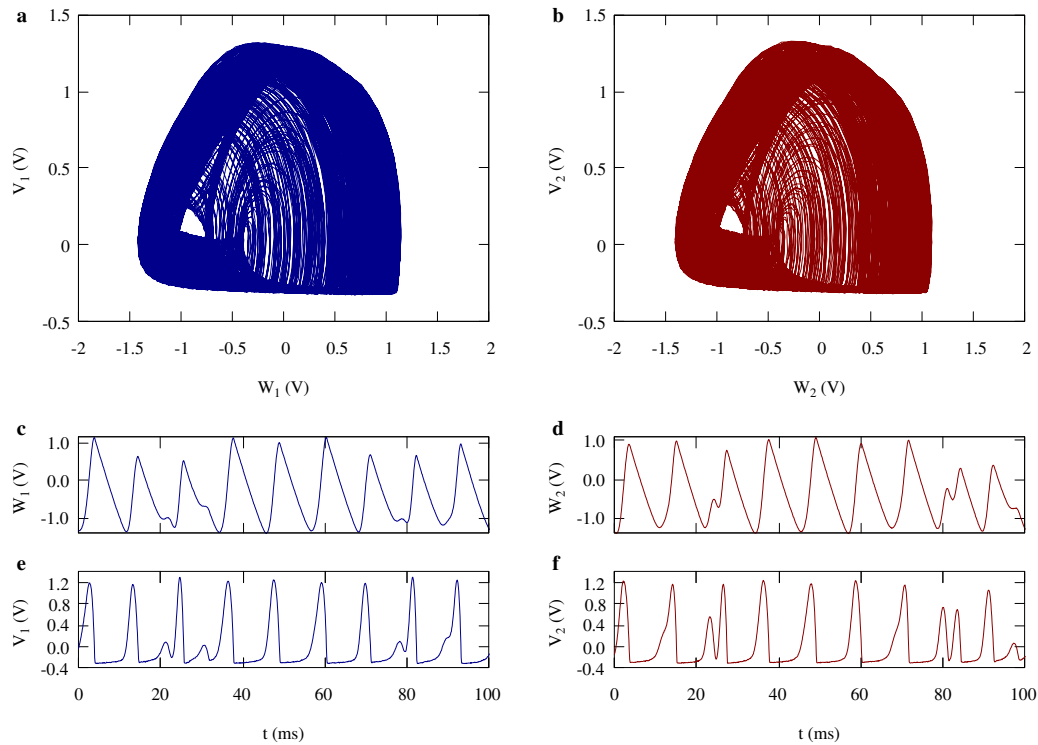


Figure 2.1: Chaotic behavior of two coupled blocks for  $V_d = 0.05$  V and for a total time of 100 ms. Phase portraits of  $V_i$  vs  $W_i$  for the first (a) and second (b) block. Time series plots for  $W_1$  (c),  $V_1$  (e),  $W_2$  (d) and  $V_2$  (f).

In order to quantify the degree of chaos of this system, it is possible to carry out

an analysis

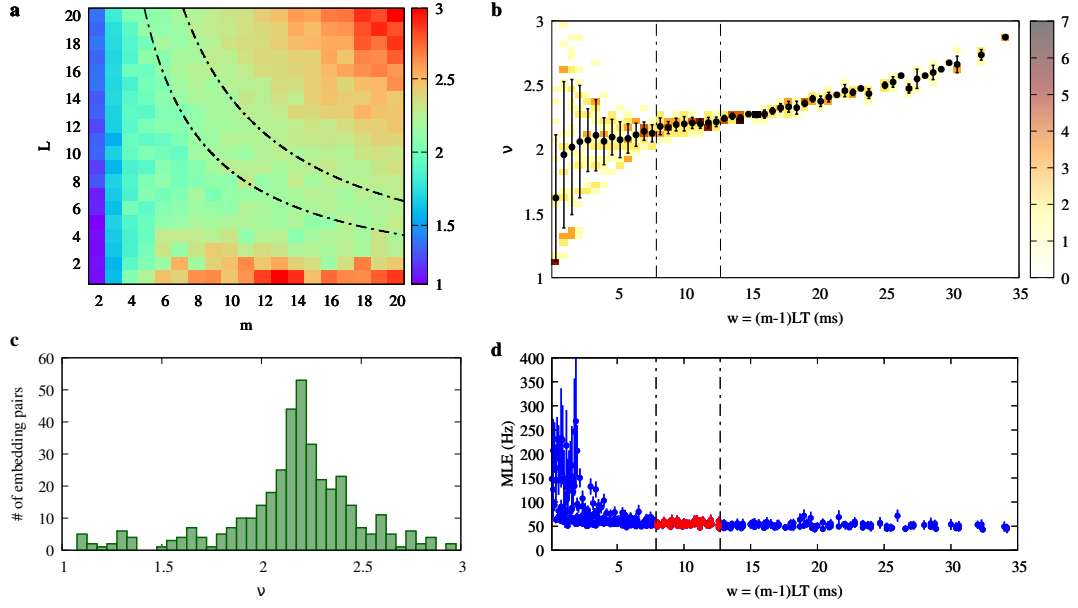


Figure 2.2: Edge

## 2.2 Three blocks

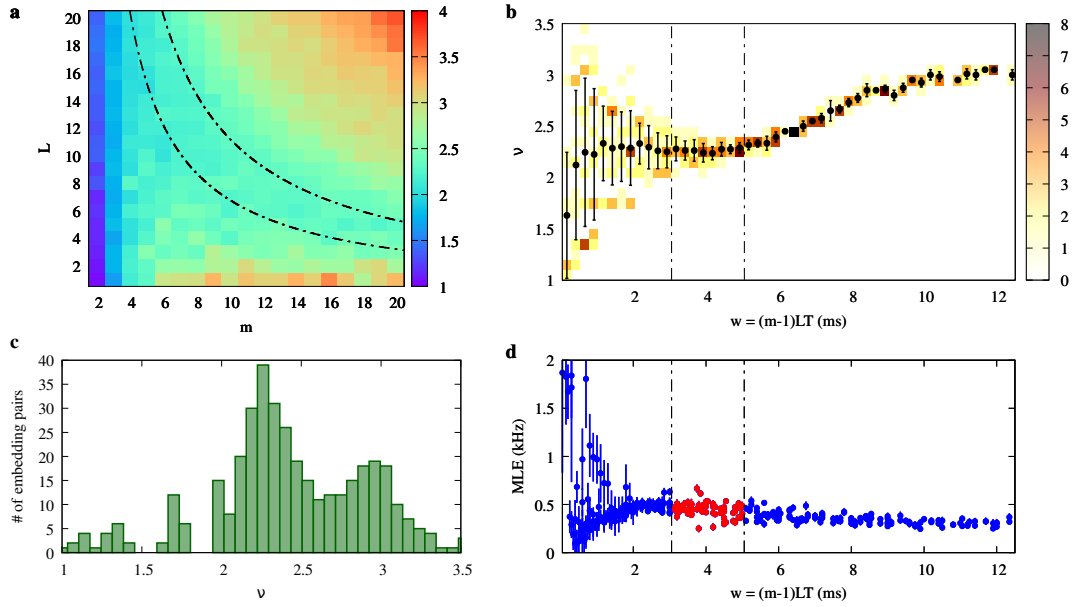


Figure 2.3: Edge

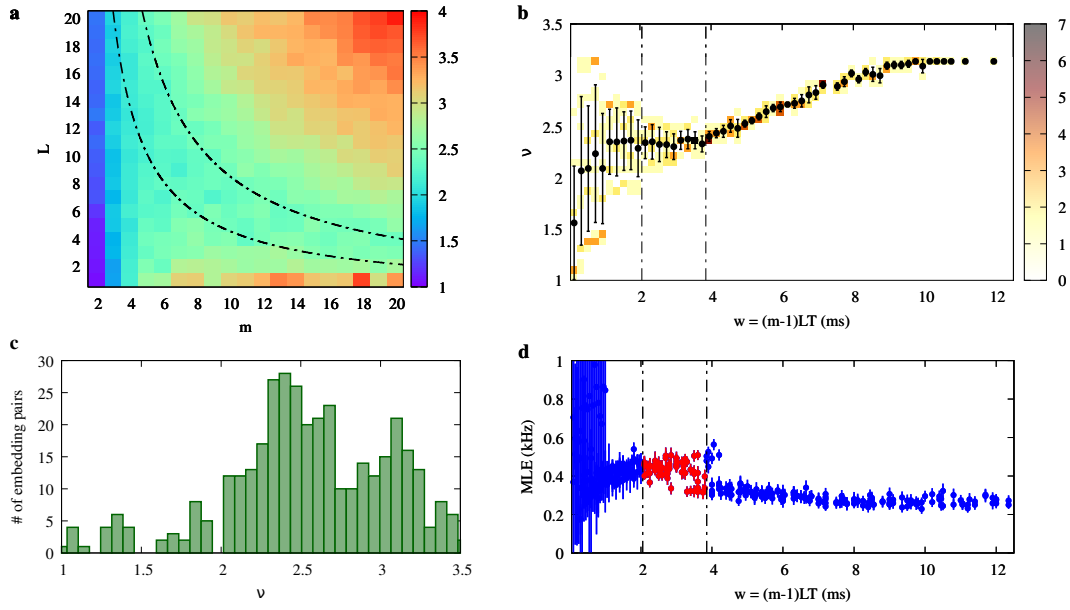


Figure 2.4: Middle

## 2.3 Four blocks

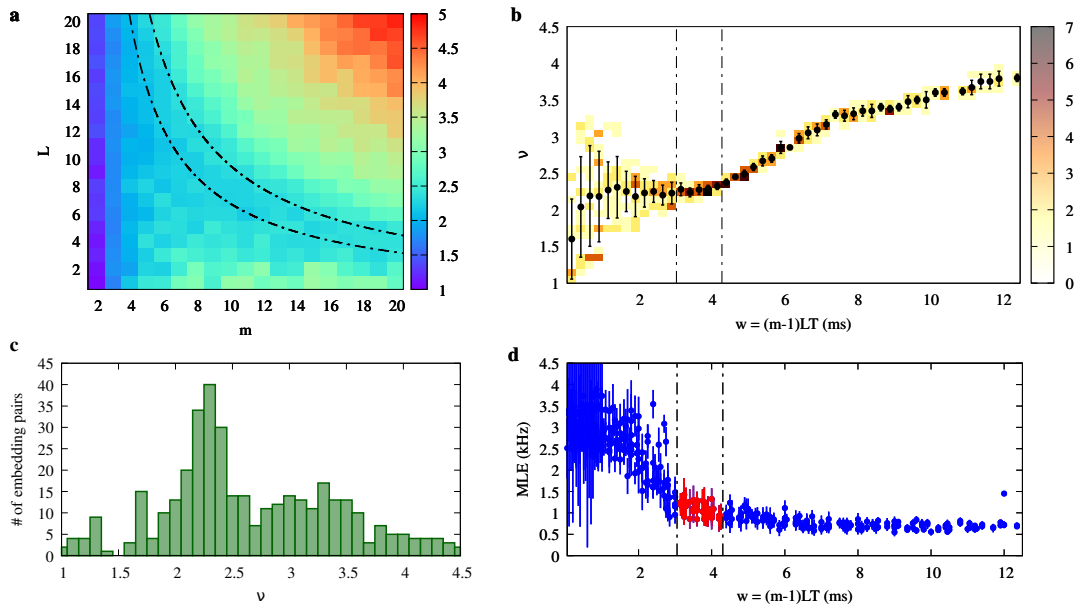


Figure 2.5: Edge

## 2.4 Five blocks

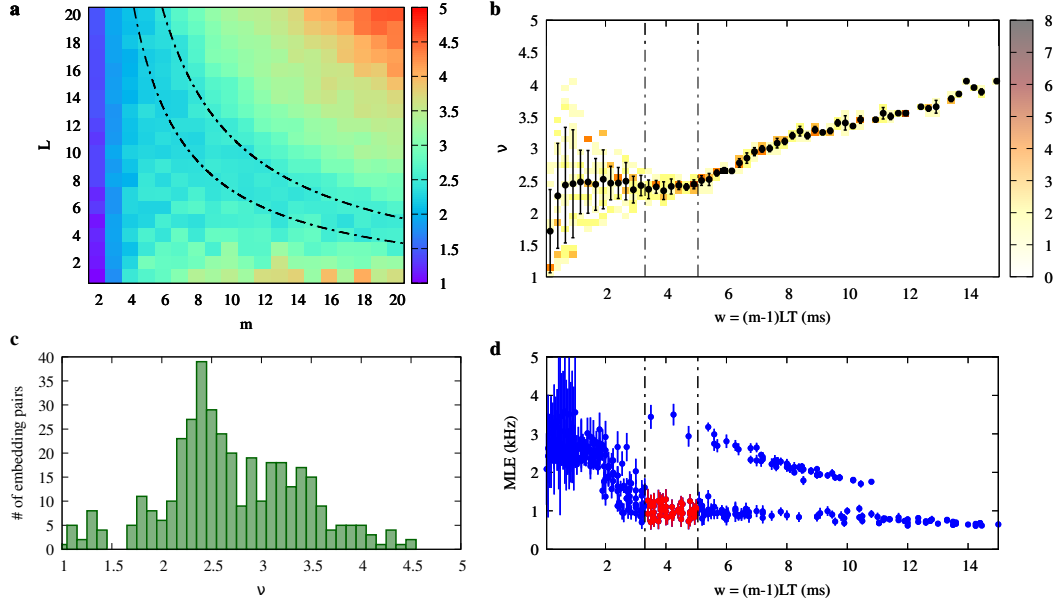


Figure 2.6: Edge

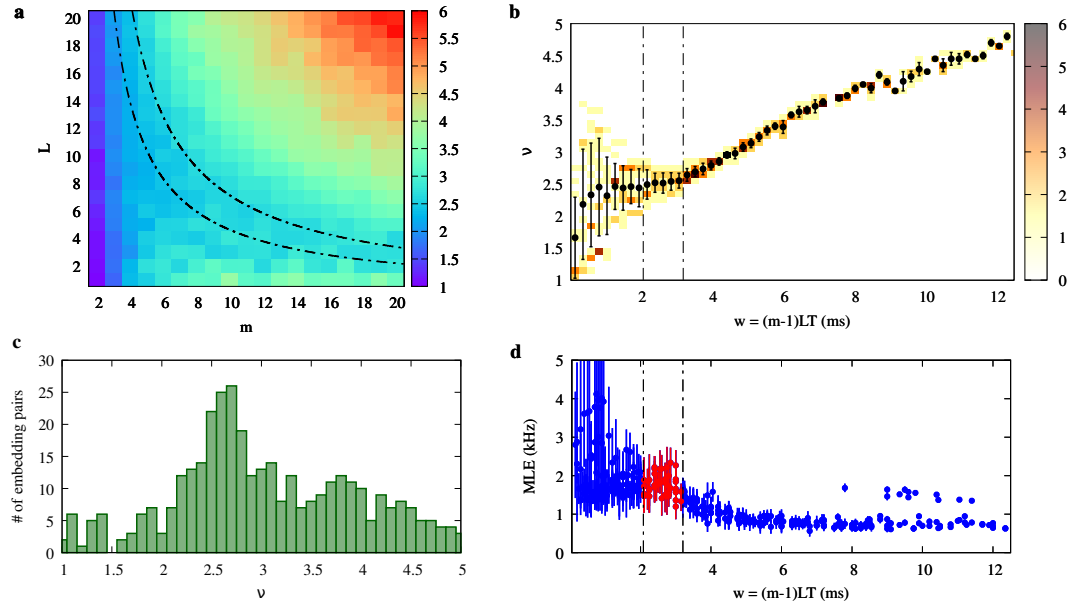


Figure 2.7: Middle

## 2.5 Six blocks

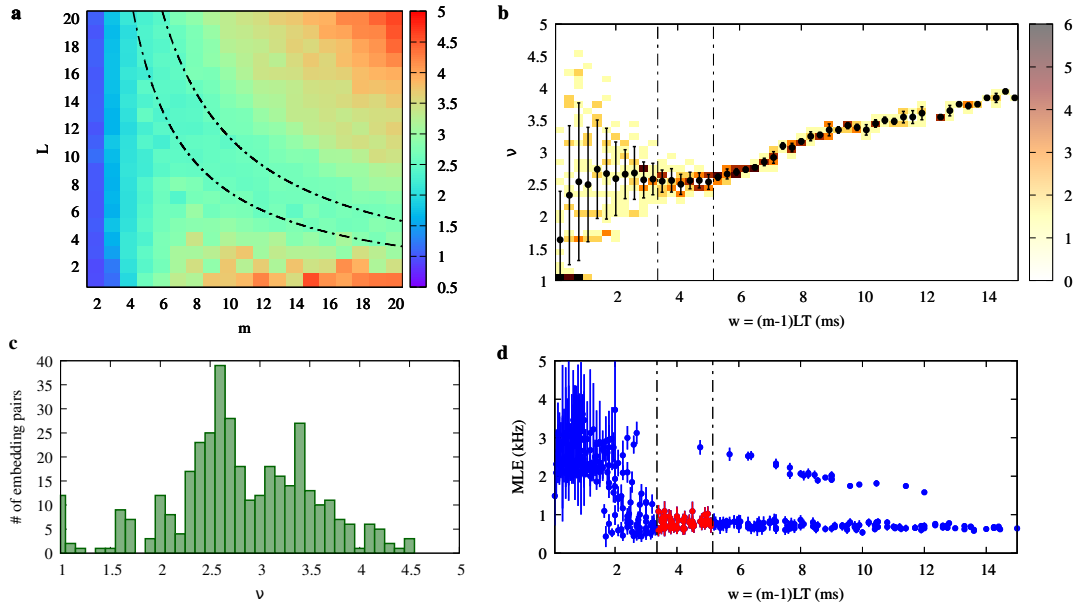


Figure 2.8: Edge

## 2.6 Seven blocks

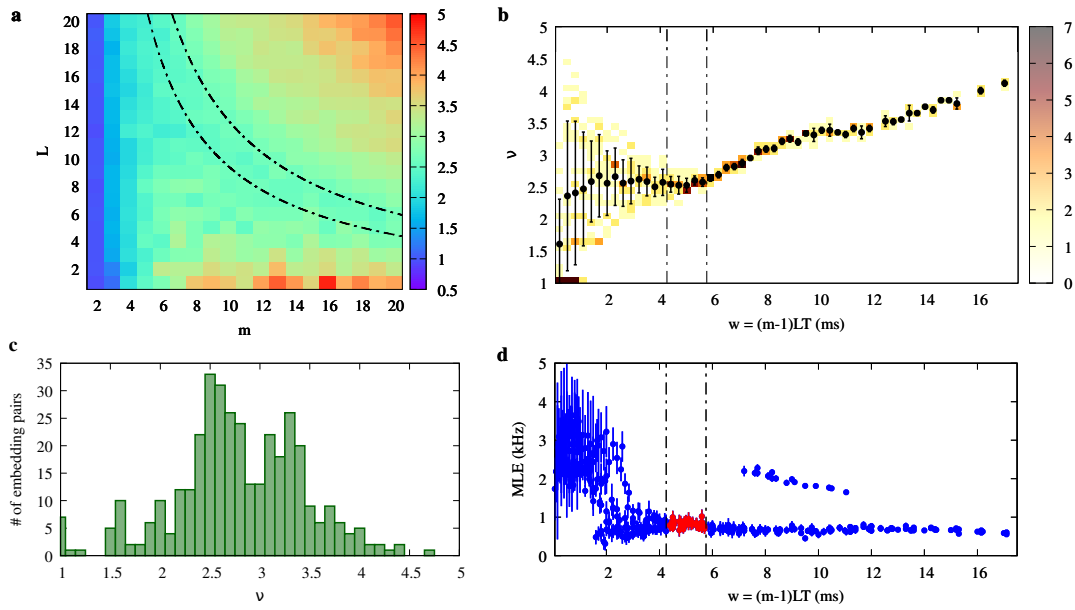


Figure 2.9: Edge

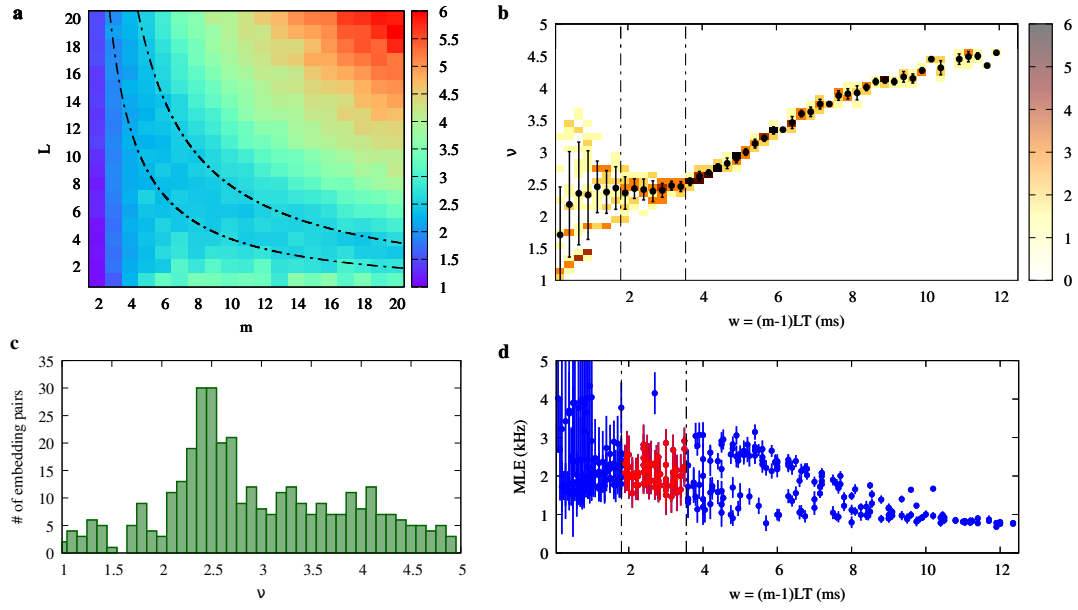


Figure 2.10: Middle

## 2.7 Eight blocks

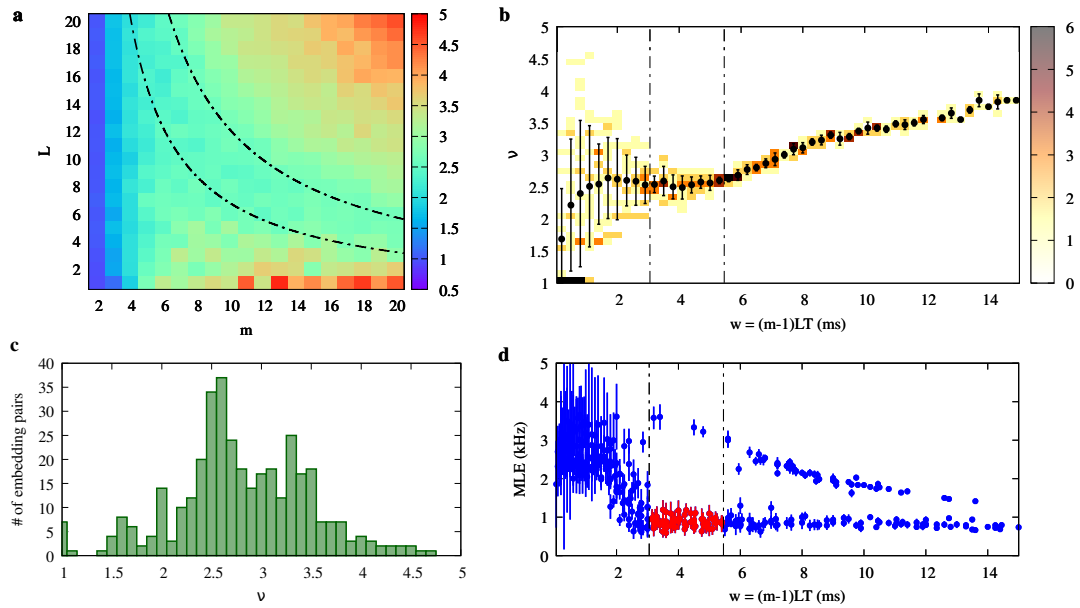


Figure 2.11: Edge

## 2.8 Nine blocks

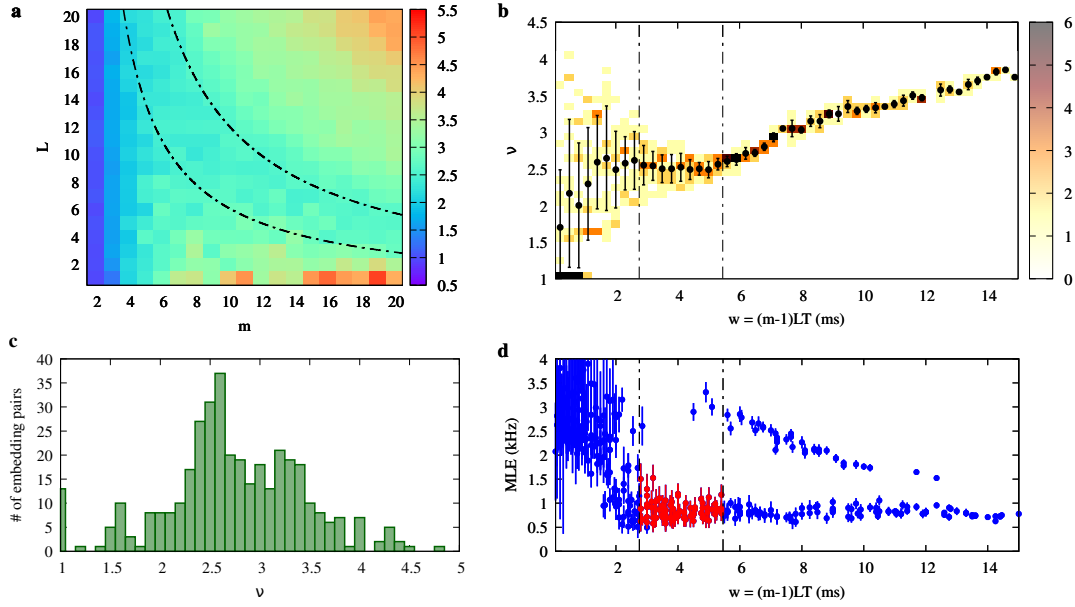


Figure 2.12: Edge

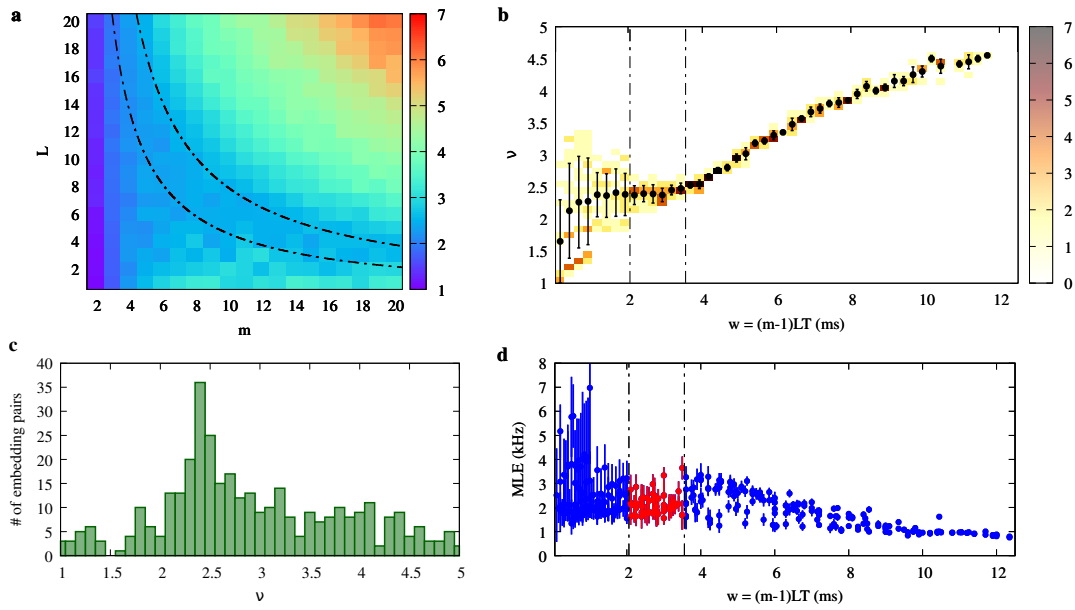


Figure 2.13: Middle



## 2.9 Ten blocks

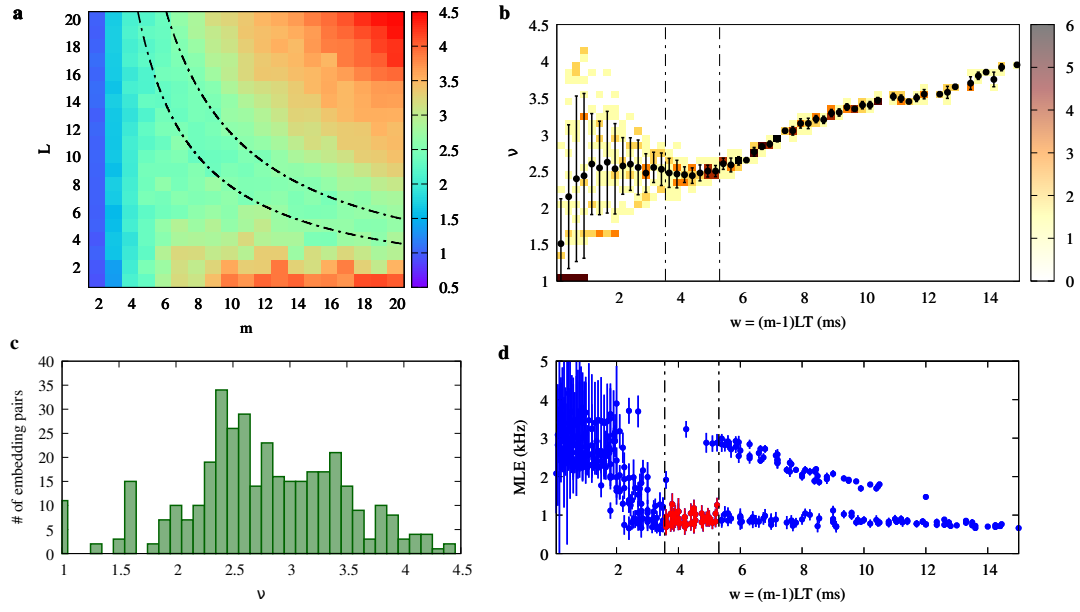


Figure 2.14: Edge

## 2.10 Conclusions

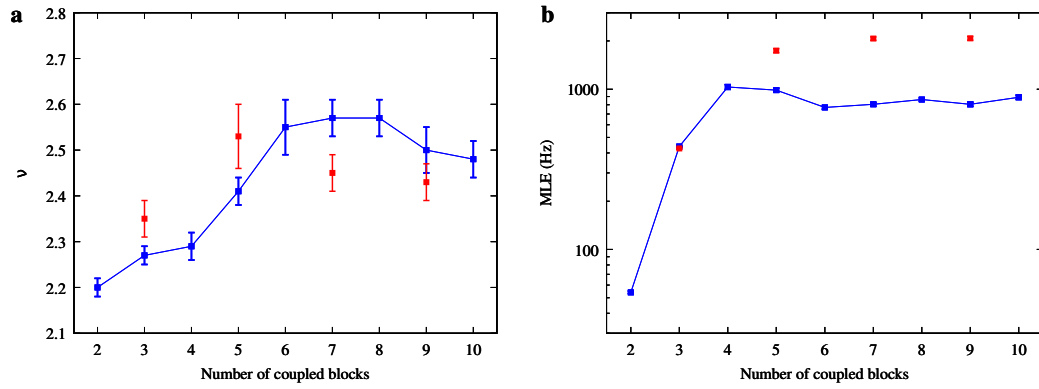


Figure 2.15: Edge (blue) and middle (red)

## Chapter 3

# Earthquake properties and statistical model of a fault



# Bibliography

- [1] R. Burridge and L. Knopoff. “Model and theoretical seismicity”. In: *Bulletin of the Seismological Society of America* (1967).
- [2] Zeev Olami, Hans Jacob S. Feder, and Kim Christensen. “Self-organized criticality in a continuous, nonconservative cellular automaton modeling earthquakes”. In: *Phys. Rev. Lett.* *68*, 1244 (1992).
- [3] A. Perinelli, R. Iuppa, and L. Ricci. “A scalable electronic analog of the Burridge–Knopoff model of earthquake faults”. In: *Chaos* *33*, 093103 (2023).
- [4] S. Field, N. Venturi, and F. Nori. “Marginal Stability and Chaos in Coupled Faults Modeled by Nonlinear Circuits”. In: *Phys. Rev. Lett.* *74* (1995).
- [5] K. Popp and P. Stelter. “Stick-slip vibrations and chaos”. In: *Philos. Trans. Roy. Soc. A* (1990).